

# Subjective and Objective Quality-of-Experience Evaluation Study for Live Video Streaming

Zehao Zhu, Wei Sun, Jun Jia, Wei Wu, Sibin Deng, Kai Li, Ying Chen, Xionguo Min, Jia Wang, Guangtao Zhai

**Abstract**—In recent years, live video streaming has gained widespread popularity across various social media platforms. Quality of experience (QoE), which reflects end-users’ satisfaction and overall experience, plays a critical role for media service providers to optimize large-scale live compression and transmission strategies to achieve perceptually optimal rate-distortion trade-off. Although many QoE metrics for video-on-demand (VoD) have been proposed, there remain significant challenges in developing QoE metrics for live video streaming. To bridge this gap, we conduct a comprehensive study of subjective and objective QoE evaluations for live video streaming. For the subjective QoE study, we introduce the first live video streaming QoE dataset, TaoLive QoE, which consists of 42 source videos collected from real live broadcasts and 1,155 corresponding distorted ones degraded due to a variety of streaming distortions, including conventional streaming distortions such as compression, stalling, as well as live streaming-specific distortions like frame skipping, variable frame rate, etc. Subsequently, a human study was conducted to derive subjective QoE scores of videos in the TaoLive QoE dataset. For the objective QoE study, we benchmark existing QoE models on the TaoLive QoE dataset as well as publicly available QoE datasets for VoD scenarios, highlighting that current models struggle to accurately assess video QoE, particularly for live content. Hence, we propose an end-to-end QoE evaluation model, Tao-QoE, which integrates multi-scale semantic features and optical flow-based motion features to predicting a retrospective QoE score, eliminating reliance on statistical quality of service (QoS) features. Extensive experiments demonstrate that Tao-QoE outperforms other models on the TaoLive QoE dataset, six publicly available QoE datasets, and eight user-generated content (UGC) video quality assessment (VQA) datasets, showcasing the effectiveness and feasibility of Tao-QoE.

**Index Terms**—quality of experience, optical flow, video quality assessment, streaming.

## I. INTRODUCTION

WITH the rapid growth of mobile devices and advancements in wireless networks in recent years, people can now watch video content on mobile devices anywhere and anytime. Streaming media technologies play an important role in ensuring that users can view such content smoothly and in real-time without waiting for complete file downloads. Specifically, the streaming media content captured by the cameras or the third-party streaming media content is encoded and segmented into data fragments. These data fragments are then transmitted to the server using appropriate transport protocols such as HTTP, HLS, RTMP, or RTSP. Users utilize client devices (e.g., mobile phones, tablets, computers, network TVs)

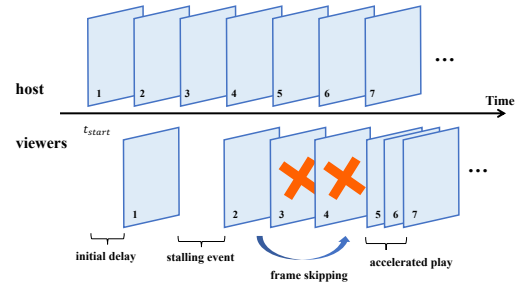


Fig. 1: Distortion in actual broadcast scenarios

to send requests over the Internet for accessing streaming media content. Upon receiving a client request, the server employs a content distribution network (CDN) to distribute the corresponding data fragment to the requesting client device. After decoding and rendering, the data is converted into audio and video content that the user can watch and listen to [1]. Video on Demand (VoD) and live streaming are two prevalent methods of streaming media technology. On the other hand, Live Streaming involves real-time transmission and display of audio or video content over the Internet, ensuring synchronized delivery for viewers to experience events as they unfold.

Limited network resources and fluctuations in client networks can result in distortions, such as degradation of video quality and stalling events, leading to a decline in the end users’ Quality of Experience (QoE). [2] Therefore, it is crucial for streaming media content providers to comprehend the factors that influence user QoE and allocate resources appropriately to enhance their satisfaction. [3] In the domain of video streaming media, Quality of Experience (QoE) is associated with numerous indicators. Among them, Video Quality Assessment (VQA) plays a pivotal role in perceiving visual quality. However, the user’s QoE is highly susceptible to disruptions such as stalling events and bit rate switching caused by network fluctuations. These factors are not evaluated by conventional VQA methods. QoE represents a comprehensive metric that encompasses video quality along with other distortions like stalling events and quality switching.

In contrast to the well-established VoD and QoE industry, the research on live streaming QoE remains insufficient, primarily due to two key factors.

- **Limited publicly available live video databases.** Current QoE databases like LIVE-NFLX and waterlooSQoE predominantly resemble VoD setups. Moreover, publicly available databases fail to accurately capture video stalling manifestations in live streaming scenarios where network

This paper was produced by the IEEE Publication Technology Group. They are in Piscataway, NJ.

Manuscript received April 19, 2021; revised August 16, 2021.

issues often result in unexpected fluctuations in frame rate and frame skipping. These distortions as shown in Fig. 1.

- **Unsatisfied qoe model mechanism.** Publicly available QoE models such as KSQI and GCNN-QoE heavily rely on statistical data (e.g., stalling time and location, bitrate), which are challenging to obtain beforehand in real-life situations, thus rendering them unsuitable for real-time live broadcast scenarios.

To address this issue, we have developed an extensive and authentic live broadcasting database known as the Tao Live QoE Database. We collect live videos from the Tao Live APP and artificially induce stalling events by manipulating the presentation time stamp (*PTS*) of the videos. It is important to note that our database encompasses various quality degradations commonly encountered in live broadcasts, including compression artifacts, stalling distortions, accelerated frame rates, and frame skipping. Furthermore, all videos in our database undergo rigorous subjective testing to obtain comprehensive retrospective QoE scores which are subsequently validated. Additionally, we introduce TAO-QoE, a pioneering deep learning-based approach capable of directly predicting QoE scores from video inputs without relying on supplementary statistics. This model performs feature extraction and fusion for assessing video presentation quality, quality switching dynamics, and occurrence of stalling events ultimately leading to retrospective QoE score predictions.

The main contributions of this work are summarized as follows:

- **We establish a large-scale live video database.** The study involved the collection of 42 high-quality videos, which were subsequently subjected to compression artifacts and stalling events by adjusting the Constant Rate Factor (*CRF*) parameters and presentation time stamp for each video frame. As a result, a total of 1,155 distorted live streaming videos were generated.
- **We carry out a well-controlled subjective experiment.** We invited 20 participants to take part in the subjective experiment, resulting in a total of 23,100 subjective annotations collected to generate the QoE scores for live videos.
- **We propose TAO-QoE, a deep learning-based model for predicting Quality of Experience (QoE) in live video streaming.** This model achieves optimal performance on public databases without the need for statistical information.

## II. RELATED WORK

### A. QoE Database

Over the past 15 years, numerous publicly available QoE databases have been developed to tackle QoE challenges. Table I illustrates common QoE databases, including WaterlooSQoE database [35]–[38] and LIVE-NFLX [39], [40], which serve as comprehensive collections of multimedia content specifically designed for evaluating QoE in diverse multimedia applications. These databases encompass a wide range of multimedia stimuli, such as images and videos, spanning different resolutions, compression levels, and content types. They also incorporate intentionally impaired content to simulate various

degradation scenarios like compression artifacts, rebuffering issues, and quality adaptation.

### B. QoE Models

In early research, video Quality of Experience (QoE) was often determined based on a set of statistical features. These studies attempted to fit certain video transmission-related metrics into a mathematical formula to predict video QoE [4]–[7]. However, the video QoE is influenced by multiple factors, including presentation quality, smoothness, video quality switching, and video stuttering. These factors are closely related to users' viewing environments, personal preferences, and perceptual abilities. Therefore, relying solely on statistical features makes it difficult to capture users' subjective experiences, and more detailed consideration of user perception and evaluation is needed. In pursuit of a better evaluation of the impact of video presentation quality on the overall Video Quality of Experience (QoE), an increasing number of studies have embraced the integration of Visual Quality Assessment (VQA) within the QoE assessment framework. Depending on the availability of reference videos during the evaluation process, video quality assessment can be classified into three categories: full-reference(FR) [8]–[12], reduced-reference(RR) [13]–[16], and no-reference(NR) approaches [17]–[24]. Both Spiteri2016 [25] and Bentalab2016 [26] regard the average bitrate of the video experienced by the user and the duration of the rebuffer events as the influencing factors of QoE. Duanmu et al. devised a QoE algorithm named SQI, which combines the FR VQA algorithm with video stalling quantification information to predict the QoE scores of videos [27]. In Video Assessment of Temporal Artifacts and Stalls (Video ATLAS) [28], Bampis et al. unify modeling of video presentation quality, stall-related features, and memory-related features of video. Subsequently, et made improvements to the SQI algorithm and developed the KSQI algorithm, which takes video presentation quality(VMAF), rebuffering, and quality adaptation (switching between profiles) into consideration [29]. With the vigorous development of deep learning technology, more and more researchers apply convolutional neural network(CNN) and recurrent neural network(RNN) to the prediction of video QoE. GCNN-QoE [30] and DA-QoE [31] both perform feature extraction and fusion on statistical features, then uses GRU to process the features and finally returns the QoE score. DeSVQ [32] feeds the high-level spatio-temporal features extracted by CNN and the low-level features measured by VQA to LSTM in turn, and finally returns the QoE score. The above three models have two common features that use statistical features and RNN. In [33], Pengfei Chen et al. constructed an end-to-end framework named TRR-QoE, which combines feature extraction, processing and QoE prediction. In Chunyi Li et al. [41] employ ResNet-50 for frame feature extraction, fuse statistics like resolution and rebuffering, and regress QoE using Support Vector Regression (SVR).

Database	Source Videos	Content type	Frame rate	Stalling manifestation	Frames Skipping	Fast playback	Total number
LIVE-NFLX-I	14	VoD	invariable	frame duplication	✗	✗	112
LIVE-NFLX-II	15	VoD	invariable	frame duplication	✗	✗	420
WaterlooSQoE-I	20	VoD	invariable	frame duplication	✗	✗	200
WaterlooSQoE-II	12	VoD	invariable	frame duplication	✗	✗	588
WaterlooSQoE-III	20	VoD	invariable	frame duplication	✗	✗	450
WaterlooSQoE-IV	5	VoD	invariable	frame duplication	✗	✗	1,350
<b>Ours</b>	42	Live video	variable	reset PTS	✓	✓	1,155

TABLE I: Comparison of QoE databases.

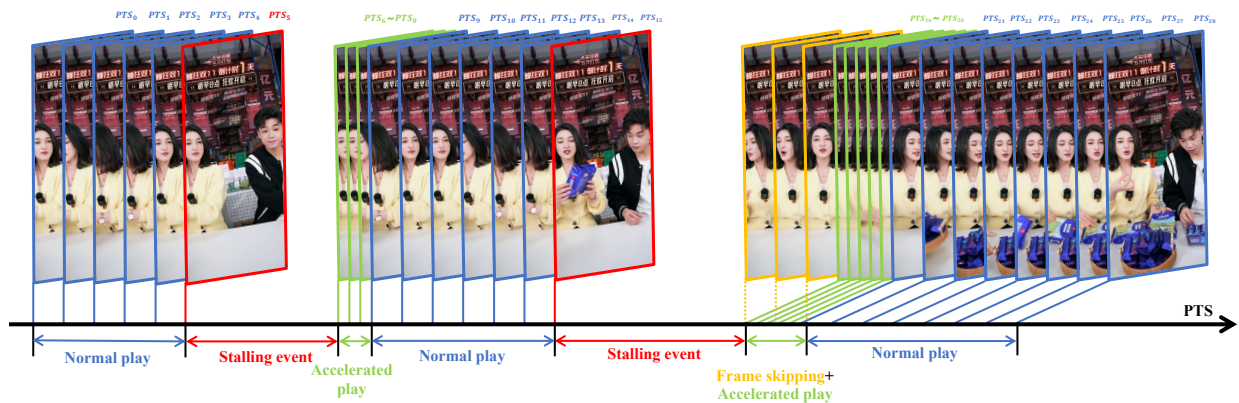


Fig. 2: Stalling event, accelerated play and frame skipping in TaoLive QoE Database.

### III. LIVE STREAMING SCENE DATABASE CONSTRUCTION

#### A. Motivation:

Despite the abundance of QoE and VQA databases, these databases suffer from certain limitations: i) insufficient diversity in source videos, resulting in a lack of complex human interaction broadcasts; ii) stalling events are predominantly represented as repeated frames, often caused by network issues leading to uneven Presentation Time Stamp (PTS) distribution; iii) live broadcast scenarios typically involve brief rebuffering periods. However, state-of-the-art QoE and VQA databases like WaterlooSQoE-III and WaterlooSQoE-IV do not encompass stalling events lasting less than one second, which is a common occurrence in real live broadcasts. Furthermore, after such stalling events in live scenarios, there is often a transition to accelerated video playback characterized by an increased frame rate or frame skipping. These variations in frame rates are not addressed in publicly available QoE databases that usually maintain a fixed frame rate.

To address these challenges, we established the TaoLive QoE database, which encompasses a larger corpus of source videos and incorporates more authentic setups involving accelerated frame rate playback, frame skipping, and other related techniques. Additionally, we manipulated PTS of video frames to accurately simulate stalling events, thereby closely resembling real-life streaming scenarios. Fig. 2 illustrates the occurrence of stalling events, accelerated frame rate playback, and frame skipping in the TaoLive QoE database. The blue video frames represent the frames played according to the source video frame rate, while the red video frames depict the displayed frames during stalling events. Additionally,

green video frames indicate fast playback (accelerated frame rate), and yellow video frames signify skipped frames due to prolonged stalling duration. Comparison between the TaoLive QoE database and other QoE databases include WaterlooSQoE database [35]–[38] and LIVE-NFLX [39], [40] is shown in Table I.

#### B. Database Construction

1) *Source Video*: We carefully selected 42 high-quality live videos encoded in H.264 from the Taobao Live app, encompassing various resolutions and frame rates. Each video has a duration of 10 seconds. To ensure optimal video performance, we excluded any videos with stall events. Specifically, we employed two resolutions (1080p and 720p) and three frame rates (20fps, 25fps, and 30fps), resulting in seven source videos for each combination of resolution and frame rate. In total, we collected a comprehensive set of 42 source videos.

2) *Distortion added*: The types of distortion we incorporated include compression, stalling events, and accelerated playback following a stall event. Due to the real-time nature of live broadcasting, once the stall event concludes, video playback resumes with certain frames being played at an accelerated rate. Frame skipping occurs when the duration of a stall event exceeds a specific threshold. The speed and duration of fast playback are generally determined by the buffer ratio on the playback side and the length of the stall event. To simulate videos with varying presentation qualities, we compressed these source videos using FFmpeg with a Constant Rate Factors (CRF) set to 15, 22, 27, 32, and 37. The 7 source videos for each frame rate are compressed based on the aforementioned 5 CRFs. Subsequently, we manually introduce

stalling, number	mode
1	1s(A1)×2, 1m(A2)×2, 1m(A2)×2, 1l(A3)×2, 1el(A4)×2
2	2s(B1), 1s+1m(B2), 1s+1l(B3), 1s+1el(B4), 2m(B5), 1m+1l(B6), 1m+1el(B7), 2l(B8)
3	3s(C1), 2s+1m(C2), 2s+1l(C3), 1s+2l(C4), 1s+1m+1l(C5)

TABLE II: 21 stalling modes.

stall events to these compressed videos. To ensure that no secondary compression occurs during the addition of stalling events, we utilize FFmpeg to modify the presentation time stamp (PTS) of the video in accordance with the designated stalling mode. This mode encompasses various combinations of stall event duration and frequency. The duration of a stall event is categorized into four levels: short (s) (0.5s or 1s), medium (m) (1.5s, 2s or 2.5s), long (l) (3s, 3.5s, 4s or 4.5s), and extra long(el) (5s, 5.5s or 6s). The maximum limit for stall event occurrences is set to 3. As depicted in Table II, there are a total of 21 combinations observed. The acceleration rate (AR) applied to expedite video playback following the termination of a stall event is configured as 1.1, 1.25, 1.5, 1.75, and 2.25.

A stall event is generated as follows.  $F = \{f_1, f_2, \dots, f_n\}$  are all video frames of compressed video.  $P = \{p_1, p_2, \dots, p_n\}$  is PTS of all compressed video frames.  $n$  is the number of compressed video frames.  $L = \{l_1, l_2, \dots, l_m\}$  is the time point when the set stall event occurs.  $T = \{t_1, t_2, \dots, t_m\}$  is the duration of stall event.  $m$  is the number of stall events. First, the index of the stall video frame is calculated according to the set time point of occurrence of the stall event and the video frame rate. The index of the stall video frame  $SF = \{sf_1, sf_2, \dots, sf_m\}$  is given by

$$sf_j = l_j \times framerate \quad j = 1, 2, \dots, m \quad (1)$$

Secondly, the PTS delay  $D = \{d_1, d_2, \dots, d_m\}$  for all video frames after this frame is calculated by

$$d_j = \frac{t_j}{timebase} \quad j = 1, 2, \dots, m \quad (2)$$

Where  $timebase$  is the time base of compressed video. The PTS delay of all video frames of the compressed video  $AD = \{ad_1, ad_2, \dots, ad_n\}$  is calculated as

$$ad_i = \begin{cases} 0 & i \leq sf_1 \\ \sum_k d_k & sf_k < i \leq sf_{k+1} \\ \sum_k^m d_k & i > sf_m \end{cases} \quad (3)$$

Where  $i$  represents the frame index of the compressed video, adjustments to certain PTS values are necessary in order to ensure smooth playback following a stall event. Specifically, the PTS interval for fast-playing video frames should be reduced based on the predetermined acceleration rate, while maintaining unchanged intervals for other video frames. The PTS interval is a constant within the FFmpeg structure AV-Packet (replaced by  $pkt.duration$  below). The frame index, PTS, and  $pkt.duration$  of the video are calculated as  $PTS = index * pkt.duration$ . The total number of accelerated playing

**Algorithm 1** The PTS calculation process of the output video

**Input:**  $P = \{p_n\}$ ;  $SF = \{sf_m\}$ ;  $D = \{d_m\}$ ;  $AD = \{ad_n\}$ ;  $QN = \{qn_m\}$ ; Total number of video frames:  $n$ ; Number of stalling events:  $m$ ; acceleration rate:  $AR; pkt.duration$ ;

**Output:**  $SP = \{sp_1, sp_2, \dots, sp_n\}$

```

1: Let  $QN\_end = [qne_1, qne_2, \dots, qne_m] = [0, \dots, 0]$ 
2: for  $i = 0; i < m - 1; i ++$  do
3:   if  $qn_i > sf_{i+1} - sf_i$  then
4:      $qne_i = sf_{i+1} - 1$ 
5:   else
6:      $qne_i = qn_{i+1} + sf_i$ 
7:   end if
8: end for
9: if  $i == m - 1$  then
10:  if  $qn_i > n - sf_i$  then
11:     $qne_i = n - 1$ 
12:  else
13:     $qne_i = qn_i + sf_i$ 
14:  end if
15: end if
16: The set of frame indexes that need to be accelerated
     $NAF = \{sf_1, \dots, qne_1, sf_m, \dots, qne_m\}$ 
17:  $sp_1 = p_1$ 
18: for  $i = 1; i < n; i ++$  do
19:  if  $i \in NAF$  then
20:     $sp_i = sp_{i-1} + pkt.duration / AR$ 
21:  else
22:     $sp_i = sp_{i-1} + pkt.duration$ 
23:  end if
24: end for
    
```

video frames following the occurrence of a stall event in this database is directly related to the duration of said stall event. It represents the cumulative count of accelerated playing video frames required to fully catch up with the live progress that was delayed due to the stall event. The total number of fast-playing video frames  $QN = \{qn_1, qn_2, \dots, qn_m\}$  is given by

$$qn_j = \frac{t_j \times AR \times framerate}{AR - 1} \quad j = 1, 2, \dots, m \quad (4)$$

The PTS interval between the current and subsequent video frames is reduced according to AR when fast forwarding, while the PTS intervals of the remaining frames remain unchanged and equal to  $pkt.duration$ . Then recalculate the PTS of the video  $SP = \{sp_1, sp_2, \dots, sp_n\}$ . Finally we add the PTS delay of all video frames  $AD = \{ad_1, ad_2, \dots, ad_n\}$  and  $SP = \{sp_1, sp_2, \dots, sp_n\}$  to get the PTS of the output videos. Then we follow Algorithm 1 to add the PTS delay of all video frames and the PTS of the source video to get the PTS of the stalled video  $SP = \{sp_1, sp_2, \dots, sp_n\}$ .

	1	1.1	1.25	1.5	1.75	2.25
1080p(1nd)	100%	-	-	-	-	-
1080p(2nd)	-	30%	30%	15%	15%	15%
720p(1st)	25%	25%	20%	15%	10 %	5%

TABLE III: AR settings for videos of different resolutions.

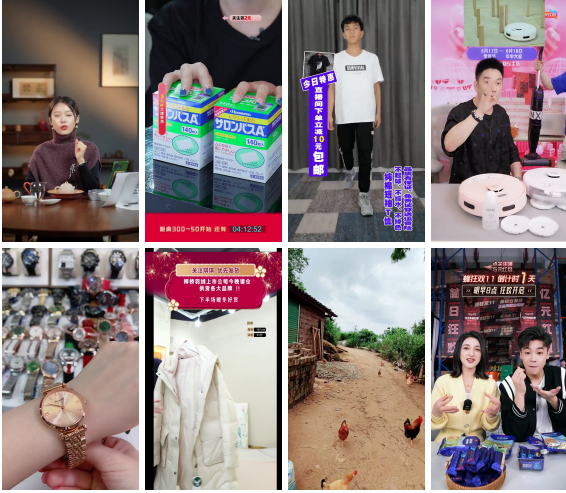


Fig. 3: Sample frames of the videos in the proposed TaoLive QoE Database.

3) *Summary*: For 7 compressed videos with different CRFs, frame rates, and resolutions, each video is subjected to 3 stall events of different modes. It should be noted that for compressed 1080p videos with stall events, AR is set to 1 during the generation of the initial batch of distorted videos with stall events. For generating the second batch of distorted 1080p videos and the first batch of 720p videos with stall events, AR is randomly assigned based on probabilities specified in Table III. The occurrence of the stall event is stochastic. A total of 945 videos exhibiting stalling events (21 1080p compressed videos  $\times$  3 stalling modes per source video  $\times$  5 CRFs  $\times$  2 batches + 21 720p compressed videos  $\times$  3 stalling modes per source video  $\times$  5 CRFs  $\times$  1 batch) are generated. A total of 210 videos without any stalling events are generated. The number of videos in the entire database is 1155. The samples of which are exhibited in Fig. 3.

### C. Subjective Experiment Methodology

In the following, we present the comprehensive methodology and configuration of the subjective test.

- **Method**: Various subjective testing methodologies have been established by ITU-R BT500-11 [42] to evaluate image quality, including single-stimulus (SS), double-stimulus impairment scale (DSIS), and paired comparison (PC). For this study, due to the short duration of the videos and retrospective scoring requirements, we utilized the SS method for our assessment.
- **QoE Rating**: The QoE scores range from 1 to 5, representing the spectrum of viewing experiences. A higher value indicates a superior quality of viewing.
- **Participants**: Before commencing the subjective testing, a training session was conducted with the subjects who then performed a subjective evaluation on a set of samples not present in the database. This facilitated familiarization of the subjects with various types of distortions contained within the video database. The Mean Opinion Score (MOS) was calculated based on subjective evaluation scores provided by 40 subjects for this sample batch, and Spearman Rank Order

Correlation Coefficient (SRCC) was computed between each subject’s evaluations and MOS. Subsequently, we selected the top 20 subjects exhibiting highest SRCC values to participate in the final round of subjective testing, comprising 11 males and 9 females.

- **Test Device**: We developed a Python-based graphical user interface (GUI) that effectively renders videos based on the specified PTS and frame rate, while also automatically collecting subjective quality scores. To mitigate geometric distortion resulting from scaling operations, we ensured playback at the video’s original resolution, with the surrounding area grayed out. The GUI was executed on a computer equipped with a 2.4 GHz Intel Core i5 processor and 16 GB of RAM. Our viewing setup comprised a 24” ViewSonic VA 2452 SM display.

## IV. DATA PROCESSING AND ANALYSIS

Based on the subjective test, we have gathered scores from all participants. Following the MOS calculation method outlined in [42]. Let  $m_{ij}$  represent the raw subjective scores assigned by participant  $i$  to video  $j$ . We calculate the z-scores using

$$z_{ij} = \frac{m_{ij} - \mu_i}{\delta_i}, \quad (5)$$

$$\mu_{ij} = \frac{1}{N_i} \sum_{j=1}^{N_i} m_{ij}, \quad (6)$$

$$\delta_i = \sqrt{\frac{1}{N_i - 1} \sum_{j=1}^{N_i} (m_{ij} - \mu_i)^2}, \quad (7)$$

where  $N_i$  denotes the number of test videos viewed by subject  $i$ .

The subject rejection procedure specified in the ITU-R BT500-11 is employed to eliminate scores from unreliable subjects [42]. Let  $z_{ij}$  denote the discarded z-scores assigned by subject  $i$  to video  $j$ . Ultimately, the z-scores are rescaled to a linear rescaling to the range [1, 5], and the Mean Opinion Score (MOS) for test video  $j$  is calculated by the averaging z-scores  $z'_{ij}$  from  $M_j$ :

$$MOS_j = \frac{1}{M_j} \sum_{i=1}^{M_j} z'_{ij} \quad (8)$$

The illustration in Fig.4 presents the MOS distributions of the proposed TaoLive QoE database from various perspectives. As depicted in Fig.4a and Fig.4c, videos with higher resolutions and frame rates exhibit correspondingly elevated QoE scores, aligning with our expectations. Notably, within the range of resolutions and frame rates present in this database, the observed differences are relatively modest. As depicted in Fig.4d, the selection of CRF parameters (15 to 22) results in a slight degradation of perceptual quality in live videos. However, when the CRF value is increased from 27 to 32, the decline in presentation quality becomes more pronounced, with most videos receiving QoE scores below 4. Furthermore, raising the CRF to 37 leads to all videos scoring below 4 on

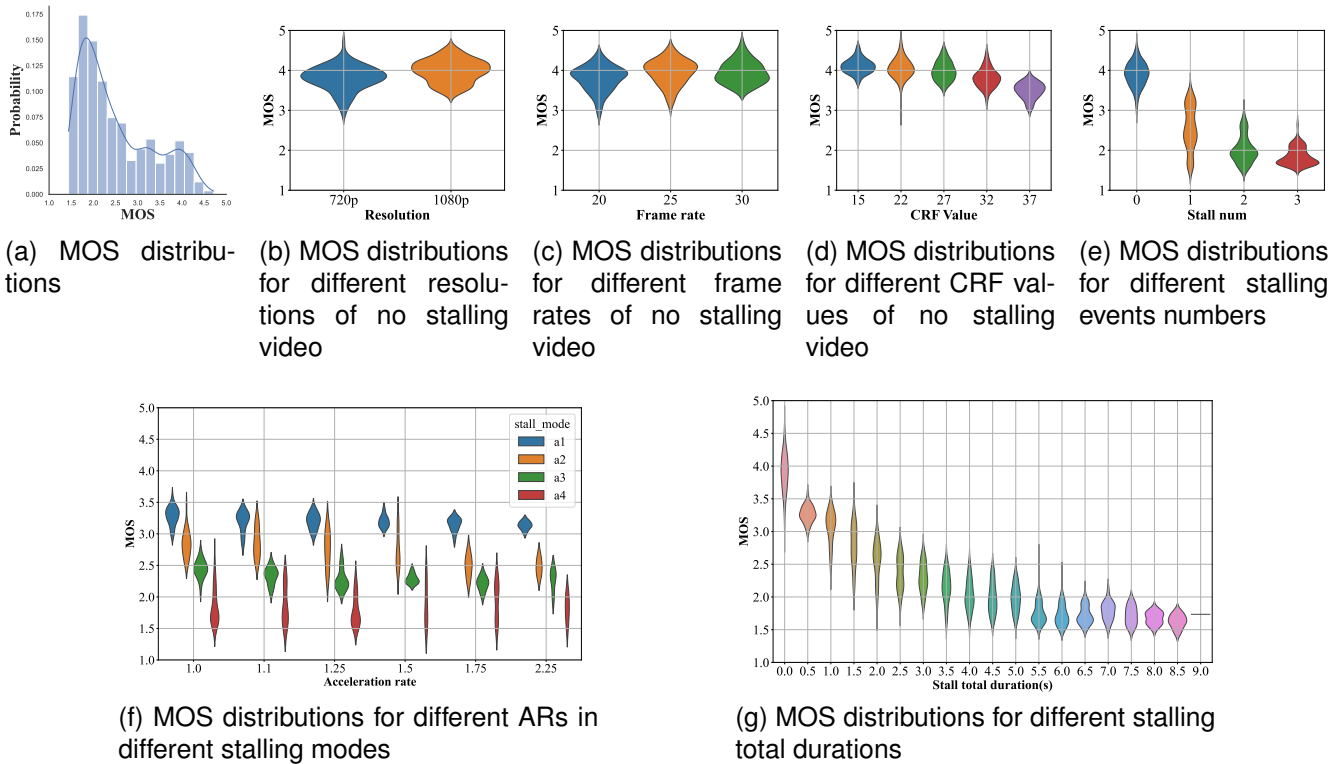


Fig. 4: Illustration of the proposed TaoLive QoE database’s MOS distributions from different perspectives

QoE assessment. These findings highlight that a CRF value of 32 or higher can significantly impair the viewing experience of the video.

As depicted in Fig.4f, the results demonstrate a negative correlation between stalling distortion and QoE score, indicating that an increase in the number of stalling events leads to a decrease in QoE score. Specifically, when the stalling event count doubles, most videos exhibit QoE scores below 2 points. Furthermore, with a threefold increase in this count, there is a further rise in the proportion of videos scoring below 2 points.

As depicted in Fig.4f, the rapid playback following a stalling event has a discernible impact on QoE. For brief stalling events (A1), the selection of AR parameters (1.1, 1.25, 1.5) results in only slight QoE degradation compared to AR=1; this loss can be considered negligible due to the short duration of fast-played video clips during such events. However, when AR exceeds 1.75, there is a noticeable decline in QoE score.

Although the duration of stalling is brief, excessively fast playback rates of video clips can result in a suboptimal viewing experience. It is noteworthy that for medium stalling events (A2), when the average rate exceeds 1.75, the quality of experience (QoE) score starts to decline sharply, surpassing the decline observed during short stalling events (A1). We hypothesize that as the duration of stalling increases, so does the time spent on fast-playing video clips, leading to a significant drop in QoE scores. For long (A3) and extra long stalling events (A4), selecting appropriate AR parameters no longer remains a crucial factor influencing the viewing experience. During this period, deterioration in viewing experience primarily depends on the duration of stalling event.

The viewing experience, as depicted in Fig.4g, exhibits a decline with an increase in the total duration of stalling. It is noteworthy that even a single instance of short stalling lasting 0.5s leads to a significant drop in QoE score (decreasing by 0.8). When the cumulative duration of stalling exceeds 5s, nearly all videos receive QoE scores below 2 points. For videos ranging from 10s to 20s in duration, a total stalling duration surpassing 5s results in an extremely poor viewing experience that viewers find difficult to tolerate.

## V. PROPOSED METHOD

The network architecture comprises five components: a video restructuring sub-network, a semantic feature extraction sub-network, a multi-scale feature fusion sub-network, a flow motion feature extraction sub-network, and a feature regression sub-network. It is shown in Fig. 5. When presented with a distorted video for evaluation, the video restructure sub-network initially analyzes the input frames to identify any stalling events caused by discontinuous PTS or accelerated playback. If such an event is detected, the corresponding stalling frames are supplemented based on the video’s frame rate and duration of the stall event. The sub-network will generate the restructured video frame sequence and its corresponding presentation timestamp (PTS). The semantic extraction sub-network aims to extract the perceived quality of all restructured video frames. Subsequently, the multi-scale quality feature fusion sub-network processes the extracted features. The flow motion feature extraction sub-network extracts flow motion features from the restructured video frames. Finally, the feature regression sub-network predicts retrospective QoE

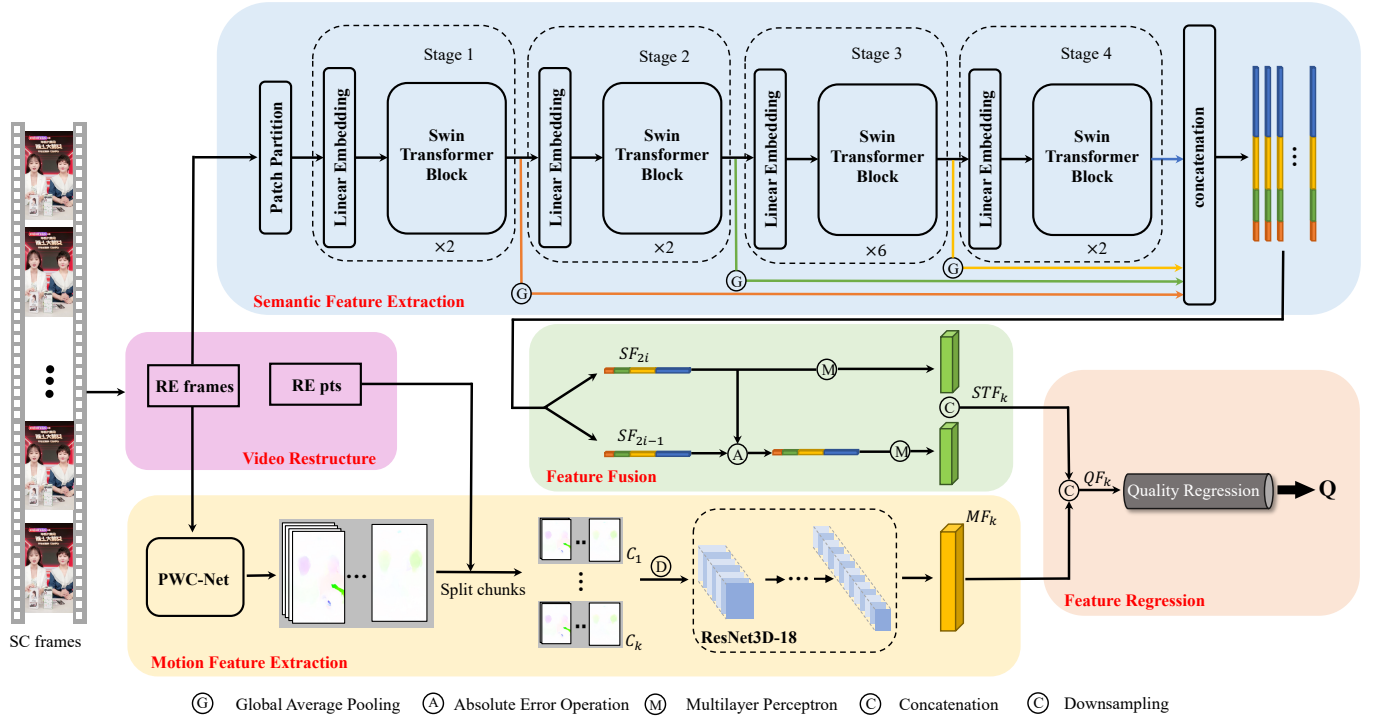


Fig. 5: The overall structure of the proposed network. 1)semantic feature extraction sub-network to extract semantic features from individual input frames; 2)flow motion feature extraction sub-network to extract flow motion features information between frames; 3)multi-scale feature fusion sub-network to process the extracted quality features; 4)feature regression sub-network to predict retrospective QoE score.

scores by integrating information from two aspects. In the following sections, we provide a detailed description of each component.

### A. Video Restructure

Mathematically, given the evaluated video chunks consists of  $N$  input frames  $F = \{f_1, f_2, \dots, f_N\}$ . We use FFmpeg to obtain the theoretical value  $\hat{P}$  of the PTS interval between frames and the PTS of all input video frames  $P = \{p_1, p_2, \dots, p_N\}$ . If the actual PTS interval between the frame  $i$  and the frame  $i+1$  exceeds the theoretical value  $\hat{P}$ , we believe that there is a stalling event between the frame  $i$  and the frame  $i+1$ , and the frame  $i$  is defined as the stalling frame. Then calculate the number of times  $rn$  the model needs to read the stalling frame repeatedly.

$$rn = \lfloor \frac{p_{i+1} - p_i}{\hat{P}} \rfloor \quad (9)$$

The process of video restructure sub-network is given in Algorithm 2.

### B. Semantic Feature Extraction

We employ the pre-trained Swin Transformer [43] as the underlying network architecture. The primary objective of the semantic feature extraction network is to acquire multi-scale semantic features for each frame. It should be noted that diverse semantic content can exert varying influences

---

#### Algorithm 2 video restructure

---

**Input:** Frames of input video  $F = \{f_1, f_2, \dots, f_N\}$ ; Total number of input video frames  $N$

**Output:** RE frames  $V = \{v_1, v_2, \dots, v_M\}$ ; PTS of RE frames  $REP = \{rep_1, rep_2, \dots, rep_M\}$

- 1: Read  $\hat{P} = pkt.duration$  by FFmpeg
  - 2: Read PTS of input video frames  $P = \{p_1, p_2, \dots, p_N\}$  by FFmpeg
  - 3: **for**  $i = 1; i < n; i++$  **do**
  - 4:      $m = 0$
  - 5:     **if**  $\hat{P} \geq p_{i+1} - p_i$  **then**
  - 6:          $v_i = f_i, rep_i = p_i$
  - 7:     **else**
  - 8:          $v_i = f_i, rep_i = p_i, rn = \lfloor \frac{p_{i+1} - p_i}{\hat{P}} \rfloor$
  - 9:         **for**  $j = 0; j < rn; j++$  **do**
  - 10:              $v_{i+j} = f_i, rep_{i+j} = p_i + \hat{P} * j$
  - 11:         **end for**
  - 12:     **end if**
  - 13: **end for**
  - 14:  $v_M = f_n, rep_m = p_N$
- 

on human tolerance towards distinct distortions [23]. Furthermore, incorporating semantic information can aid in detecting and measuring perceptual distortions, making it a reasonable addition to the assessment of presentation quality. Additionally, presentation quality is hierarchical in nature,

with perception occurring from low-level features to high-level ones. To account for this hierarchy, we splice multi-scale features extracted by the four stages of Swin Transformer and use them as frame-level semantic features.

Mathematically, given the evaluated video consists of  $2L$  input frames, we feed these RE frames  $V = \{v_1, v_2, \dots, v_{2L}\}$  into the semantic feature extraction network.  $SF = \{SF_1, SF_2, \dots, SF_{2L}\}$  is the output multi-scale semantic features.

$$SF_i = \alpha_1 \oplus \alpha_2 \oplus \alpha_3 \oplus \alpha_4 \quad i = 1, 2, \dots, 2L \quad (10)$$

$$\alpha_j = GAP(L_j(v_i)) \quad j = 1, 2, 3, 4 \quad (11)$$

where  $SF_i$  indicates the extracted semantic features from  $i$ -th frame  $v_i$ .  $GAP(\cdot)$  represents the global average pooling operation.  $L_j(v_i)$  is the feature of the  $j$ -th stage output of Swin Transformer.  $\alpha_j$  denotes the average pooled features from  $L_j(v_i)$ .

### C. Flow Motion Feature Extraction

Live broadcasts are often affected by unstable shooting environments and restricted network conditions, resulting in motion distortions such as jitter and stagnant events. Therefore, relying solely on semantic features at the frame level is insufficient to accurately capture these distortions. While some videos may exhibit high presentation quality, the presence of jitter and stalling events significantly diminishes the Quality of Experience (QoE) for such live broadcasts. Hence, it is imperative to incorporate motion features in QoE prediction models. To detect stalling events effectively, we initially segment the extracted optical flow based on the Presentation Time Stamp (PTS) of Reference Frames (RE frames), with each segment having a duration of 1 second. Subsequently, inter-frame optical flow images are extracted from each segment using a pretrained PWC-Net [44].

$$C_k = \Gamma(V_i) \quad i = 1, 2, \dots, M \quad (12)$$

where  $C_k$  represents the extraction and clipping operations of inter-frame optical flow images for RE frames. We employ PTS to perform the clipping operation on inter-frame optical flow images. In case of accelerated video playback, the number of optical flow images contained in  $C_k$  may vary.

Subsequently, the inter-frame optical flow images are resampled at a rate of 16fps for each clip, followed by leveraging a pre-trained 3D-CNN backbone ResNet-18 [45] to capture motion distortion at the clip level.

$$MF_k = \Phi(C_k) \quad k = 1, 2, \dots, 2L/r \quad (13)$$

The flow motion features extracted from clip  $C_k$  are denoted as  $MF_k$ , where  $\Gamma(\cdot)$  represents the operation of extracting flow and  $\Phi(\cdot)$  represents the operation of extracting flow motion features.

### D. Multi-scale Feature Fusion

The evidence from [47] demonstrates that there exists an inverse relationship between video quality and adaptation quality, where lower adaptation quality contributes to a more enjoyable viewing experience for the audience. Consequently, the absolute error of semantic features between consecutive frames can serve as an indicator of adaptation quality.

$$SF'_{2m} = |SF_{2m} - SF_{2m-1}| \quad m = 1, 2, \dots, L \quad (14)$$

where  $SF'_{2m}$  represent the absolute error between adjacent semantic features. Then the multi-scale fusion can be derived as:

$$STF_{2m} = W(\varphi(SF_{2m}) \oplus \varphi(SF'_{2m})) \quad m = 1, 2, \dots, L \quad (15)$$

where  $\oplus(\cdot)$  stands for the concatenation operation,  $\varphi(\cdot)$  represents the learnable Multilayer Perceptron (MLP).  $W$  is a learnable linear mapping operation, and we finally obtain the spatio-temporal fused features  $STF_k$ . Then we connect the spatio-temporal fusion feature and the flow motion feature to get the final QoE feature.

$$QF_k = STF_k \oplus \varphi(MF_k) \quad k = 1, 2, \dots, L \quad (16)$$

### E. Feature Regression

After the aforementioned process of feature extraction and fusion, we employ a fully connected layer to perform regression on the QoE features in order to obtain clip-level QoE scores.

$$Q_k = FC(QF_k) \quad k = 1, 2, \dots, L \quad (17)$$

where  $FC(\cdot)$  is the fully-connected layers and  $Q_i$  presents the QoE score of clip  $C_k$ . Finally, we average all clips of the input video to obtain a retrospective QoE score for that video.

$$Q = \frac{r}{n} \sum_1^{\frac{n}{r}} Q_k \quad (18)$$

where  $Q$  is the video QoE score and  $\frac{n}{r}$  stands for the number of clips. We simply use the Mean Squared Error (MSE) as the loss function:

$$Loss = \frac{1}{n} \sum_{i=1}^n (Q_g - Q_p)^2 \quad (19)$$

where  $n$  indicates the number of videos in a mini-batch,  $Q_g$  and  $Q_p$  are the MOS and predicted retrospective QoE score respectively.

## VI. EXPERIMENT

In this section, we initially provide a comprehensive description of the experimental setup. Subsequently, we evaluate the performance of our proposed TAO-QoE model and compare it with other prominent QoE models using our Tao Live QoE Database as well as publicly available QoE and VQA databases. Furthermore, ablation experiments are conducted to investigate the individual contributions of different sub-modules towards enhancing the overall model performance.



TABLE IV: Comparison of QoE models. Best in **red** and second in **blue**

Models		Mok2011	FTW	Liu2012	Xue2014	P.1203	Bentaleb	Spiteri	SQI	KSQI	ASPECT	GCNN-QoE	Tao-QoE
Databases	Criteria												
LIVE-II	PLCC	0.614	0.470	0.794	0.761	0.654	0.903	0.790	0.904	0.863	0.667	<b>0.935</b>	<b>0.948</b>
	SRCC	0.594	0.464	0.793	0.754	0.693	0.895	0.773	0.902	0.862	0.606	<b>0.927</b>	<b>0.946</b>
	RMSE	0.610	0.501	0.456	0.468	0.565	<b>0.322</b>	0.477	0.323	0.363	0.581	/	<b>0.250</b>
	KRCC	0.477	0.363	0.604	0.584	0.529	0.740	0.581	0.748	0.703	0.425	<b>0.778</b>	<b>0.800</b>
Waterloo-I	PLCC	0.478	0.488	0.596	0.781	0.561	0.920	0.834	0.799	0.909	0.790	<b>0.945</b>	<b>0.933</b>
	SRCC	0.452	0.465	0.711	0.856	0.737	0.919	0.861	0.791	0.903	0.774	<b>0.934</b>	<b>0.929</b>
	RMSE	17.552	17.152	14.285	9.962	12.865	<b>7.250</b>	9.409	11.308	7.813	11.598	/	<b>7.163</b>
	KRCC	0.363	0.369	0.528	0.679	0.558	0.758	0.683	0.615	0.738	0.594	<b>0.806</b>	<b>0.775</b>
Waterloo-II	PLCC	0.190	0.364	0.592	0.423	0.773	0.838	<b>0.846</b>	0.685	0.691	0.803	0.826	<b>0.874</b>
	SRCC	0.173	0.305	0.595	0.433	0.801	0.818	<b>0.820</b>	0.722	0.531	0.790	0.818	<b>0.866</b>
	RMSE	13.991	14.041	10.048	13.622	9.554	7.820	<b>7.953</b>	10.766	10.307	9.665	/	<b>6.645</b>
	KRCC	0.131	0.211	0.435	0.292	0.620	0.637	<b>0.634</b>	0.531	0.383	0.605	0.624	<b>0.680</b>
Waterloo-III	PLCC	0.302	0.423	0.606	0.481	0.782	0.855	0.820	0.723	0.682	0.798	<b>0.890</b>	<b>0.900</b>
	SRCC	0.270	0.378	0.623	0.469	0.809	0.836	0.804	0.744	0.500	0.762	<b>0.881</b>	<b>0.890</b>
	RMSE	13.444	13.459	9.989	12.828	9.219	<b>7.364</b>	8.246	9.947	10.291	8.954	/	<b>6.494</b>
	KRCC	0.204	0.260	0.455	0.318	0.626	0.650	0.613	0.552	0.355	0.569	<b>0.707</b>	<b>0.711</b>
Waterloo-IV	PLCC	0.084	0.193	0.415	0.178	0.765	0.710	0.733	0.716	0.595	0.626	<b>0.855</b>	<b>0.865</b>
	SRCC	0.038	0.150	0.527	0.254	0.785	0.694	0.714	0.696	0.508	0.542	<b>0.846</b>	<b>0.858</b>
	RMSE	14.413	14.337	11.382	14.055	9.324	10.219	<b>9.311</b>	10.159	11.424	11.450	/	<b>7.069</b>
	KRCC	0.031	0.116	0.374	0.182	0.608	0.499	0.532	0.501	0.357	0.398	<b>0.668</b>	<b>0.674</b>
TLQD	PLCC	0.612	0.734	0.575	0.779	0.910	0.814	0.842	0.876	0.758	<b>0.915</b>	/	<b>0.959</b>
	SRCC	0.535	0.660	0.578	0.767	0.868	0.837	0.870	0.858	0.709	<b>0.891</b>	/	<b>0.925</b>
	RMSE	0.612	0.555	0.509	0.501	0.299	0.324	0.298	0.345	0.530	<b>0.301</b>	/	<b>0.230</b>
	KRCC	0.470	0.541	0.449	0.571	0.695	0.665	0.702	0.678	0.558	<b>0.680</b>	/	<b>0.769</b>
W.A.	PLCC	0.380	0.445	0.596	0.567	0.741	<b>0.840</b>	0.811	0.784	0.750	0.767	/	<b>0.913</b>
	SRCC	0.344	0.404	0.638	0.589	0.782	<b>0.833</b>	0.807	0.785	0.669	0.728	/	<b>0.902</b>
	RMSE	10.104	10.008	7.778	8.573	6.971	<b>5.550</b>	5.952	7.141	6.788	7.092	/	<b>4.642</b>
	KRCC	0.279	0.310	0.474	0.438	0.606	<b>0.658</b>	0.624	0.604	0.516	0.545	/	<b>0.735</b>

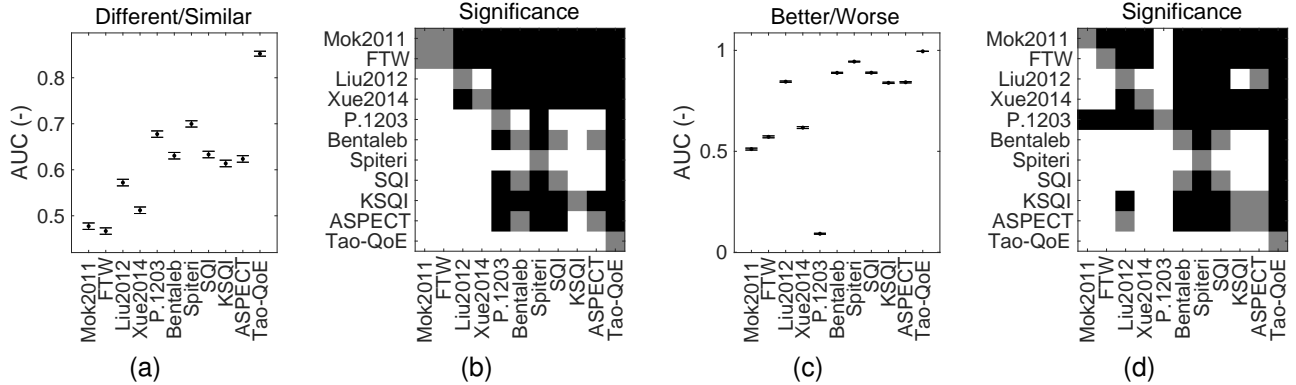


Fig. 6: New criteria performance of 11 state-of-art FR and NR QoE models and our proposed model on WaterlooSqE-IV database. (a) and (b) are the different vs. similar ROC analysis results. (c) and (d) are the better vs. worse analysis results. Note that a white/black square in (b) and (d) means the row metric is statistically better/worse than the column one. A gray square means the row method and the column method are statistically indistinguishable.

### A. Implementation Details

The Tao-QoE model is implemented in PyTorch [51], with the Swin Transformer backbone utilizing pretrained weights from the ImageNet-1K database [48] for semantic feature extraction. Additionally, the ResNet3D-18 employs pretrained weights from the Kinetics-400 database [49]. The weights of both the multi-scale feature fusion sub-network and sub-feature regression are initialized randomly. Regarding the semantic feature extraction sub-network, it operates at the original resolution ( $1920 \times 1080$  or  $1280 \times 960$ ) of input video frames. The flow motion feature extraction sub-network involves the extraction of optical flow maps from video frames at their original resolution, followed by resizing the optical flow map to  $224 \times 224$  and inputting it into a ResNet-18 3D-CNN. Our model was trained and tested on a server equipped with an Intel(R) Xeon(R) Platinum 8163 CPU @ 2.50GHz,

128GB RAM, and NVIDIA Tesla V100 SXM2. The Adam optimizer [50] is utilized with an initial learning rate of 0.001. In case the training loss fails to decrease within 5 epochs, the learning rate is halved. The default number of epochs is set to 50. During the process of flow motion feature extraction, all videos are down-sampled to a frame rate of 16fps for ensuring consistent feature dimensions. Following standard practice, we split the database into train and test sets at an 80%-20% ratio. To assess the stability of the QoE model, we randomly perform 10 content-based splits and record their average result as the final performance. Specifically, for the WaterlooSqE-IV database, we performed content-based splitting five times due to the limited availability of only 5 source videos in the database.

TABLE V: Comparison of VQA models. Best in **red** and second in **blue**

Models		TLVQM	VSFA	SimpleVQA	FastVQA	Tao-QoE
Databases	Criteria					
LIVE-Qualcomm	PLCC	0.625	0.461	<b>0.783</b>	0.584	<b>0.802</b>
	SRCC	0.599	0.458	<b>0.758</b>	0.547	<b>0.768</b>
	RMSE	9.017	7.293	<b>7.100</b>	9.014	<b>6.848</b>
	KRCC	0.453	0.330	<b>0.573</b>	0.385	<b>0.580</b>
CVD2014	PLCC	0.771	0.449	<b>0.890</b>	0.850	<b>0.906</b>
	SRCC	0.751	0.347	<b>0.875</b>	0.843	<b>0.898</b>
	RMSE	13.925	18.548	<b>9.694</b>	12.619	<b>9.038</b>
	KRCC	0.565	0.246	<b>0.703</b>	0.651	<b>0.728</b>
KoNViD-1k	PLCC	0.843	0.774	<b>0.845</b>	0.759	<b>0.868</b>
	SRCC	0.810	0.768	<b>0.842</b>	0.759	<b>0.867</b>
	RMSE	0.355	0.413	<b>0.349</b>	0.459	<b>0.324</b>
	KRCC	0.615	0.572	<b>0.651</b>	0.569	<b>0.679</b>
VDPVE	PLCC	0.577	0.534	<b>0.726</b>	0.592	<b>0.749</b>
	SRCC	0.573	0.513	<b>0.724</b>	0.622	<b>0.753</b>
	RMSE	11.321	11.127	<b>9.277</b>	11.422	<b>8.956</b>
	KRCC	0.406	0.365	<b>0.532</b>	0.436	<b>0.555</b>
LIVE-VQC	PLCC	<b>0.789</b>	0.765	0.747	0.709	<b>0.869</b>
	SRCC	<b>0.786</b>	0.737	0.716	0.695	<b>0.857</b>
	RMSE	<b>10.708</b>	11.061	11.471	13.222	<b>8.537</b>
	KRCC	<b>0.595</b>	0.544	0.527	0.512	<b>0.680</b>
MSU	PLCC	0.411	0.582	<b>0.789</b>	0.631	<b>0.805</b>
	SRCC	0.391	0.528	<b>0.767</b>	0.609	<b>0.777</b>
	RMSE	2.719	1.101	<b>1.039</b>	1.332	<b>1.010</b>
	KRCC	0.280	0.399	<b>0.589</b>	0.438	<b>0.584</b>
YouTubeUGC	PLCC	0.624	0.513	<b>0.812</b>	0.535	<b>0.854</b>
	SRCC	0.662	0.532	<b>0.815</b>	0.536	<b>0.852</b>
	RMSE	0.537	0.535	<b>0.381</b>	0.654	<b>0.340</b>
	KRCC	0.472	0.383	<b>0.621</b>	0.370	<b>0.662</b>
LIVE-WC	PLCC	0.823	0.589	<b>0.922</b>	0.764	<b>0.945</b>
	SRCC	0.824	0.597	<b>0.921</b>	0.773	<b>0.942</b>
	RMSE	8.998	10.517	<b>5.537</b>	9.203	<b>4.706</b>
	KRCC	0.638	0.463	<b>0.756</b>	0.575	<b>0.794</b>
W.A.	PLCC	0.683	0.583	<b>0.814</b>	0.678	<b>0.850</b>
	SRCC	0.674	0.560	<b>0.802</b>	0.673	<b>0.839</b>
	RMSE	7.197	7.574	<b>0.606</b>	7.241	<b>4.970</b>
	KRCC	0.503	0.413	<b>0.619</b>	0.492	<b>0.658</b>

TABLE VI: Experimental performance of the ablation study of QoE databases. Best in **red** and second in **blue**. S, F, FM, M represent semantic feature extraction sub-network, multi-scale feature fusion sub-network, flow motion feature extraction sub-network, motion feature extraction sub-network respectively. ALL represents S+FM+F.

Models		S	S+F	FM	S+FM	S+F+M	ALL
Databases	Criteria						
LIVE-NFLX-II	PLCC	<b>0.912</b>	0.773	0.858	0.909	0.835	<b>0.948</b>
	SRCC	<b>0.904</b>	0.778	0.832	0.908	0.810	<b>0.946</b>
	RMSE	<b>0.304</b>	0.441	0.394	0.323	0.420	<b>0.250</b>
	KRCC	<b>0.746</b>	0.618	0.659	0.743	0.651	<b>0.800</b>
Waterloo-I	PLCC	0.874	0.907	0.704	<b>0.925</b>	0.900	<b>0.933</b>
	SRCC	0.869	0.909	0.686	<b>0.926</b>	0.891	<b>0.929</b>
	RMSE	9.622	8.353	13.861	<b>7.514</b>	8.438	<b>7.163</b>
	KRCC	0.688	0.743	0.515	<b>0.777</b>	0.724	<b>0.775</b>
Waterloo-II	PLCC	0.800	<b>0.868</b>	0.762	0.809	0.814	<b>0.874</b>
	SRCC	0.797	<b>0.861</b>	0.730	0.796	0.793	<b>0.866</b>
	RMSE	7.867	<b>6.716</b>	8.647	7.779	7.908	<b>6.645</b>
	KRCC	0.614	<b>0.678</b>	0.554	0.607	0.604	<b>0.680</b>
Waterloo-III	PLCC	0.751	<b>0.899</b>	0.642	0.867	0.886	<b>0.900</b>
	SRCC	0.628	<b>0.884</b>	0.511	0.847	0.873	<b>0.890</b>
	RMSE	9.697	<b>6.529</b>	11.329	7.386	6.837	<b>6.494</b>
	KRCC	0.468	<b>0.706</b>	0.372	0.658	0.695	<b>0.711</b>
Waterloo-IV	PLCC	0.814	<b>0.855</b>	0.806	0.843	0.847	<b>0.865</b>
	SRCC	0.791	<b>0.847</b>	0.779	0.831	0.835	<b>0.858</b>
	RMSE	8.221	<b>7.241</b>	8.366	7.523	7.362	<b>7.069</b>
	KRCC	0.604	<b>0.664</b>	0.609	0.645	0.643	<b>0.674</b>
TLVD	PLCC	0.908	0.923	0.694	<b>0.947</b>	0.938	<b>0.959</b>
	SRCC	0.865	0.875	0.650	<b>0.921</b>	0.912	<b>0.925</b>
	RMSE	0.398	0.314	0.585	<b>0.266</b>	0.300	<b>0.230</b>
	KRCC	0.643	0.702	0.473	<b>0.764</b>	0.755	<b>0.769</b>

B. Benchmark Databases & Compared Models

We compared the currently available QoE and VQA models on the QoE and VQA database respectively. In the field of QoE, we selected TaoLive QoE Database and five other available QoE databases, including LIVE-NFLX-II [40], WaterlooSQoE-I [35], WaterlooSQoE-II [36], WaterlooSQoE-III [37] and WaterlooSQoE-IV [38]. We compare the proposed model with the following QoE models:

- Traditional models: P.1203 [34], SQI [29], Bentaleb2016 [26], Spiteri2016 [26], VideoATLAS [28], KSQI [29]
- Deep learning models: GCNN-QoE [30], ASPECT [41]

Unfortunately, the code for the GCNN model is not publicly available, thus hindering our ability to assess its performance on TaoLive QoE database.

In the domain of VQA, we selected 8 UGC VQA databases: LIVE-Qualcomm [52], CVD2014 [53], KoNViD-1k [54], VDPVE [55], LIVE-VQC [57], MSU [56], YouTubeUGC [58], LIVE-WC [59].

We compare the proposed method with the following non-reference models: LTVQM [69], VSFA [70], SimpleVQA [71], FastVQA [72].

C. Criteria

Two types of evaluation criteria are employed to assess the performance of models. The first criterion, known as the Video

TABLE VII: Experimental performance of the ablation study of VQA databases. Best in **red** and second in **blue**. S, F, FM, M represent semantic feature extraction sub-network, multi-scale feature fusion sub-network, flow motion feature extraction sub-network, motion feature extraction sub-network respectively. ALL represents S+FM+F.

Models		S	S+F	FM	S+FM	S+F+M	ALL
Databases	Criteria						
LIVE-Qualcomm	PLCC	0.776	0.785	0.621	<b>0.808</b>	0.728	<b>0.802</b>
	SRCC	0.730	0.737	0.525	<b>0.777</b>	0.678	<b>0.768</b>
	RMSE	7.183	7.057	8.895	<b>6.721</b>	7.778	<b>6.848</b>
	KRCC	0.553	0.556	0.378	<b>0.584</b>	0.506	<b>0.580</b>
CVD2014	PLCC	0.856	0.877	0.774	<b>0.895</b>	0.867	<b>0.906</b>
	SRCC	0.839	0.860	0.745	<b>0.885</b>	0.852	<b>0.898</b>
	RMSE	10.871	10.100	12.943	<b>9.495</b>	10.448	<b>9.038</b>
	KRCC	0.656	0.681	0.550	<b>0.704</b>	0.668	<b>0.728</b>
KoNViD-1k	PLCC	0.749	0.753	0.552	<b>0.768</b>	0.849	<b>0.868</b>
	SRCC	0.753	0.755	0.545	<b>0.772</b>	0.847	<b>0.867</b>
	RMSE	8.956	8.889	11.285	<b>8.675</b>	0.345	<b>0.324</b>
	KRCC	0.555	0.559	0.376	<b>0.573</b>	0.655	<b>0.679</b>
VDPVE	PLCC	0.749	<b>0.753</b>	0.552	<b>0.768</b>	0.723	0.749
	SRCC	0.753	<b>0.755</b>	0.545	<b>0.772</b>	0.721	0.753
	RMSE	8.956	<b>8.889</b>	11.285	<b>8.675</b>	9.328	8.956
	KRCC	0.555	<b>0.559</b>	0.376	<b>0.573</b>	0.525	0.555
LIVE-VQC	PLCC	0.792	0.821	0.746	<b>0.867</b>	0.823	<b>0.869</b>
	SRCC	0.751	0.792	0.718	<b>0.852</b>	0.798	<b>0.857</b>
	RMSE	10.464	9.821	11.469	<b>8.597</b>	9.749	<b>8.537</b>
	KRCC	0.558	0.600	0.538	<b>0.673</b>	0.607	<b>0.680</b>
MSU	PLCC	0.696	0.766	0.647	<b>0.784</b>	0.725	<b>0.805</b>
	SRCC	0.660	0.722	0.573	<b>0.759</b>	0.670	<b>0.777</b>
	RMSE	1.208	1.083	1.286	<b>1.051</b>	1.139	<b>1.010</b>
	KRCC	0.498	0.555	0.423	<b>0.568</b>	0.536	<b>0.584</b>
YouTubeUGC	PLCC	0.816	0.824	0.649	<b>0.846</b>	0.816	<b>0.854</b>
	SRCC	0.812	0.821	0.612	<b>0.843</b>	0.811	<b>0.852</b>
	RMSE	0.377	0.371	0.498	<b>0.349</b>	0.378	<b>0.340</b>
	KRCC	0.617	0.627	0.438	<b>0.651</b>	0.618	<b>0.662</b>
LIVE-WC	PLCC	<b>0.938</b>	0.935	0.698	0.930	0.921	<b>0.945</b>
	SRCC	<b>0.935</b>	0.932	0.685	0.927	0.918	<b>0.942</b>
	RMSE	<b>4.969</b>	5.114	10.091	5.269	5.484	<b>4.706</b>
	KRCC	<b>0.780</b>	0.773	0.507	0.771	0.758	<b>0.794</b>

Quality Experts Group (VQEG) criteria [60]–[62], calculates a series of correlation values between predicted scores and Mean Opinion Scores (MOSs). The second criterion, proposed by Krasula et al. [63]–[66], evaluates the classification abilities of models in distinguishing between two videos based on their quality. We refer to the first criterion as VQEG criteria and the second one as classification criteria.

For VQEG criteria, the model prediction scores should be initially mapped using the following function:

$$f(p) = \xi_1 \left( \frac{1}{2} - \frac{1}{1 + e^{\xi_2(p - \xi_3)}} \right) + \xi_4 p + \xi_5 \quad (20)$$

where  $\{\xi_i | i = 1, 2, 3, 4, 5\}$  is the parameter to be fitted,  $p$  and  $f(p)$  represent the prediction score and mapping score respectively. The mapped scores are then used to calculate four correlation values with MOSs, namely Spearman Rank-Order Correlation Coefficient (SRCC), Pearson Linear Correlation Coefficient (PLCC), Root Mean Squared Error (RMSE), and Kendall Rank-order Correlation Coefficient (KRCC). These statistical indices serve different purposes in assessing model performance. Specifically, PLCC reflects the linearity of algorithm predictions, SRCC indicates their monotonicity or predictive correlation, while RMSE evaluates model consistency. An excellent model should achieve values close to 1 for SRCC, PLCC and KRCC.

For the classification criteria, we adhere to the procedures outlined in [60] and employ statistical methods from [67] to analyze subjective data for determining the significance of differences between each pair of stimuli. A confidence level of 95% is set. The entire dataset is partitioned into subsets based on significant differences and similarities. In a

significantly distinct subset, we partition the stimulus pairs into groups based on positive and negative differences in MOS. A higher ability to discriminate dissimilar/similar pairs and superior/inferior stimulus pairs indicates better model performance. Therefore, we employ the area under the ROC curve (AUC) as an evaluation metric for assessing classification performance of models. Furthermore, we compare AUC values obtained from different models to determine if there are statistically significant disparities in their performances [68].

We use the VQEG standard to analyze the performance of the Tao-QoE model and other VQA models on different UGC databases. Since the VQA database selected in this paper does not disclose the standard deviation of the annotation scores for each video, we are unable to calculate the classification criteria. In the case of QoE models, adhering to standard practices [46], we utilize both VQEG criteria and Classification criteria for evaluating the effectiveness of Tao-QoE and other QoE models on the QoE database.

#### D. QoE Performance

1) *VQEG Criteria*: The experimental performance on 6 QoE databases is presented in Table IV. The following conclusions can be drawn from the results. (1) Our proposed Tao-QoE model demonstrates the best performance among all models. Specifically, on the largest publicly available database, WaterlooSQoE-IV, SRCC and PLCC improve by 0.012 and 0.010, respectively. (2) Traditional QoE algorithms perform significantly worse than deep learning models on WaterlooSQoE-III, WaterlooSQoE-IV, and LIVE-NFLX-II databases due to the presence of various distortion types such as quality switching and rebuffering. Deep learning models have an advantage in perceiving these distortions compared to traditional models. (3) Unfortunately, we were unable to obtain the performance of GCNN-QoE on TaoLive QoE Database since it is not available. However, it is evident that our model can accurately evaluate the QoE of live videos compared with traditional QoE algorithms.

2) *Classification Criteria*: We present the performance evaluation based on the classification criteria of all the aforementioned QoE models using the largest publicly available database, WaterlooSQoE-IV, as shown in Fig 6. From this figure, we can draw similar conclusions to those derived from the VQEG performance. Firstly, our proposed model Tao-QoE outperforms other QoE models by a significant margin in both the 'Different vs. Similar' and 'Better vs. Worse' classification tasks. Statistical analysis also demonstrates that our proposed model is significantly superior to other models on the WaterlooSQoE-IV database. Secondly, the AUC values for the 'Better vs. Worse' classification task are consistently higher than those for the 'Different vs. Similar' classification task, indicating that the latter is more challenging and there is still room for improvement in this area.

#### E. VQA Performance

We present the VQEG performance on 8 UGC VQA databases in Table V. Several observations can be made.

Firstly, our proposed Tao-QoE model achieves the highest performance among all models. Particularly, on the three recently introduced larger-scale UGC databases (MSU, YouTubeUGC, and LIVE-WC), our model demonstrates significantly improved performance compared to other models. Secondly, it is evident that deep learning models hold an advantage over traditional models, which aligns with the findings of the QoE experiment.

#### F. Ablation Study

1) *QoE*: To evaluate the contributions of different features and sub-networks in Tao-QoE, we conduct ablation experiments. The experimental results of QoE are shown in Table VI. Firstly, combining features yield better performance than using a single group of features and employing all features leads to the best performance among the combinations of different features. In addition, models that use semantic features achieve better performance, while models that do not use semantic features (such as FM) perform poorly, which proves that semantic features contribute the most to the final performance. Secondly, Compare the final model(ALL: S+FM+F) with the model without optical flow(S+F+M, M represents the extraction of motion features directly from the video clip instead of the optical flow clip), using optical flow motion features will significantly improve QoE prediction. The QoE database contains more inter-frame distortions, such as stalling distortion. Optical flow can perceive the movement of pixels between two frames, which is very helpful for perceiving stalling distortion. Thirdly, Since the multi-scale feature fusion sub-network performs differential operations on the frame-level semantic features, the multi-scale feature fusion sub-network has a certain ability to perceive the quality switching distortion in the QoE field. The results in the Table VI show that the performance of using the multi-scale feature fusion sub-network is significantly improved compared to not using the sub-network(such as S and S+F, S+F and ALL).

2) *VQA*: The experimental results of QoE are shown in Table VII. Firstly, although the VQA database does not include complex distortions such as stalling distortion and quality switching, the model using all features (ALL) still shows good performance. Secondly, on the VQA database, the multi-scale feature fusion sub-network does not contribute as much to the performance as on the QoE database. This is because the VQA database does not include quality switching distortions, and the semantic feature extraction sub-network is basically competent for the task of extracting video quality. Thirdly, the flow motion feature still contributes to the prediction of video quality(such as S and S+FM, S+F+M and ALL).

## VII. CONCLUSION

In this paper, we construct a database Taolive QoE Database for large-scale live broadcast scenes. Taolive QoE Database selects 42 high-quality videos as the original video, and adds distortion by changing the CRF parameters and the PTS of the video frame. Meanwhile we conduct a subjective experiment to collect the QoE scores of these videos. Furthermore, we propose a QoE model to evaluate the QoE of videos from both

semantic and motion aspects. Extensive experimental results confirm the effectiveness of the proposed method.

## REFERENCES

- [1] Hamilton, William A., Oliver Garretson, and Andruid Kerne. "Streaming on twitch: fostering participatory communities of play within live mixed media." Proceedings of the SIGCHI conference on human factors in computing systems. 2014.
- [2] Akhtar, Zahid, et al. "Why is multimedia quality of experience assessment a challenging problem?." IEEE Access 7 (2019): 117897-117915.
- [3] Brunnström, Kjell, et al. "Qualinet white paper on definitions of quality of experience." (2013).
- [4] Brunnström, Kjell, et al. "Qualinet white paper on definitions of quality of experience." (2013).
- [5] Mok, Ricky KP, Edmond WW Chan, and Rocky KC Chang. "Measuring the quality of experience of HTTP video streaming." 12th IFIP/IEEE international symposium on integrated network management (IM 2011) and workshops. IEEE, 2011.
- [6] Xue, Jingteng, et al. "Assessing quality of experience for adaptive HTTP video streaming." 2014 IEEE International Conference on Multimedia and Expo Workshops (ICMEW). IEEE, 2014.
- [7] Yin, Xiaoqi, et al. "A control-theoretic approach for dynamic adaptive video streaming over HTTP." Proceedings of the 2015 ACM Conference on Special Interest Group on Data Communication. 2015.
- [8] Manasa, K., and Sumohana S. Channappayya. "An optical flow-based full reference video quality assessment algorithm." IEEE Transactions on Image Processing 25.6 (2016): 2480-2492.
- [9] Wu, Jinjian, et al. "Quality assessment for video with degradation along salient trajectories." IEEE Transactions on Multimedia 21.11 (2019): 2738-2749.
- [10] Bampis, Christos G., Zhi Li, and Alan C. Bovik. "Spatiotemporal feature integration and model fusion for full reference video quality assessment." IEEE Transactions on Circuits and Systems for Video Technology 29.8 (2018): 2256-2270.
- [11] Wang, Zhou, Ligang Lu, and Alan C. Bovik. "Video quality assessment based on structural distortion measurement." Signal processing: Image communication 19.2 (2004): 121-132.
- [12] Seshadrinathan, Kalpana, and Alan Conrad Bovik. "Motion tuned spatio-temporal quality assessment of natural videos." IEEE transactions on image processing 19.2 (2009): 335-350.
- [13] Soundararajan, Rajiv, and Alan C. Bovik. "Video quality assessment by reduced reference spatio-temporal entropic differencing." IEEE Transactions on Circuits and Systems for Video Technology 23.4 (2012): 684-694.
- [14] Wang, Zhou, and Eero P. Simoncelli. "Reduced-reference image quality assessment using a wavelet-domain natural image statistic model." Human vision and electronic imaging X. Vol. 5666. SPIE, 2005.
- [15] Ma, Lin, et al. "Reduced-reference image quality assessment using reorganized DCT-based image representation." IEEE Transactions on multimedia 13.4 (2011): 824-829.
- [16] Rehman, Abdul, and Zhou Wang. "Reduced-reference image quality assessment by structural similarity estimation." IEEE transactions on image processing 21.8 (2012): 3378-3389.
- [17] Men, Hui, Hanhe Lin, and Dietmar Saupe. "Empirical evaluation of no-reference VQA methods on a natural video quality database." 2017 Ninth international conference on quality of multimedia experience (QoMEX). IEEE, 2017.
- [18] Men, Hui, Hanhe Lin, and Dietmar Saupe. "Spatiotemporal feature combination model for no-reference video quality assessment." 2018 Tenth international conference on quality of multimedia experience (QoMEX). IEEE, 2018.
- [19] Li, Yuming, et al. "No-reference video quality assessment with 3D shearlet transform and convolutional neural networks." IEEE Transactions on Circuits and Systems for Video Technology 26.6 (2015): 1044-1057.
- [20] Saad, Michele A., Alan C. Bovik, and Christophe Charrier. "Blind prediction of natural video quality." IEEE Transactions on image processing 23.3 (2014): 1352-1365.
- [21] Xu, Jingtao, et al. "No-reference video quality assessment via feature learning." 2014 IEEE international conference on image processing (ICIP). IEEE, 2014.
- [22] Mittal, Anish, Michele A. Saad, and Alan C. Bovik. "A completely blind video integrity oracle." IEEE Transactions on Image Processing 25.1 (2015): 289-300.

- [23] Li, Dingquan, Tingting Jiang, and Ming Jiang. "Quality assessment of in-the-wild videos." *Proceedings of the 27th ACM International Conference on Multimedia*. 2019.
- [24] Chen, Pengfei, et al. "RIRNet: Recurrent-in-recurrent network for video quality assessment." *Proceedings of the 28th ACM international conference on multimedia*. 2020.
- [25] Spiteri, Kevin, Rahul Uргаonkar, and Ramesh K. Sitaraman. "BOLA: Near-optimal bitrate adaptation for online videos." *IEEE/ACM transactions on networking* 28.4 (2020): 1698-1711.
- [26] Bentaleb, Abdelhak, Ali C. Begen, and Roger Zimmermann. "SD-NDASH: Improving QoE of HTTP adaptive streaming using software defined networking." *Proceedings of the 24th ACM international conference on Multimedia*. 2016.
- [27] Duanmu, Zhengfang, et al. "A quality-of-experience index for streaming video." *IEEE Journal of Selected Topics in Signal Processing* 11.1 (2016): 154-166.
- [28] Bampis, Christos G., and Alan C. Bovik. "Learning to predict streaming video QoE: Distortions, rebuffering and memory." *arXiv preprint arXiv:1703.00633* (2017).
- [29] Duanmu, Zhengfang, et al. "A knowledge-driven quality-of-experience model for adaptive streaming videos." *arXiv preprint arXiv:1911.07944* (2019).
- [30] Zhou, Zhiming, et al. "Quality of Experience Evaluation for Streaming Video Using CGNN." *2020 IEEE International Conference on Visual Communications and Image Processing (VCIP)*. IEEE, 2020.
- [31] Li, Leida, et al. "From Whole Video to Frames: Weakly-Supervised Domain Adaptive Continuous-Time QoE Evaluation." *IEEE Transactions on Image Processing* 31 (2022): 4937-4951.
- [32] Ghosh, Monalisa, Dr Chetna Singhal, and Rushikesh Woyal. "DeSVQ: Deep learning based streaming video QoE estimation." *Proceedings of the 23rd International Conference on Distributed Computing and Networking*. 2022.
- [33] Chen, Pengfei, et al. "Temporal reasoning guided QoE evaluation for mobile live video broadcasting." *IEEE Transactions on Image Processing* 30 (2021): 3279-3292.
- [34] Raake, Alexander, et al. "A bitstream-based, scalable video-quality model for HTTP adaptive streaming: ITU-T P. 1203.1." *2017 Ninth international conference on quality of multimedia experience (QoMEX)*. IEEE, 2017.
- [35] Duanmu, Zhengfang, et al. "A quality-of-experience index for streaming video." *IEEE Journal of Selected Topics in Signal Processing* 11.1 (2016): 154-166.
- [36] Duanmu, Zhengfang, Kede Ma, and Zhou Wang. "Quality-of-experience for adaptive streaming videos: An expectation confirmation theory motivated approach." *IEEE Transactions on Image Processing* 27.12 (2018): 6135-6146.
- [37] Duanmu, Zhengfang, Abdul Rehman, and Zhou Wang. "A quality-of-experience database for adaptive video streaming." *IEEE Transactions on Broadcasting* 64.2 (2018): 474-487.
- [38] Duanmu, Zhengfang, et al. "Assessing the quality-of-experience of adaptive bitrate video streaming." *arXiv preprint arXiv:2008.08804* (2020).
- [39] Bampis, Christos George, et al. "Study of temporal effects on subjective video quality of experience." *IEEE Transactions on Image Processing* 26.11 (2017): 5217-5231.
- [40] Bampis, Christos G., et al. "Towards perceptually optimized end-to-end adaptive video streaming." *arXiv preprint arXiv:1808.03898* (2018).
- [41] Li, Chunyi, et al. "A real-time blind quality-of-experience assessment metric for HTTP adaptive streaming." *arXiv preprint arXiv:2303.09818* (2023).
- [42] BT, RIR. "Methodology for the subjective assessment of the quality of television pictures." *International Telecommunication Union* 4 (2002).
- [43] Liu, Ze, et al. "Swin transformer: Hierarchical vision transformer using shifted windows." *Proceedings of the IEEE/CVF international conference on computer vision*. 2021.
- [44] Sun, Deqing, et al. "Pwc-net: Cnns for optical flow using pyramid, warping, and cost volume." *Proceedings of the IEEE conference on computer vision and pattern recognition*. 2018.
- [45] Hara, Kensho, Hirokatsu Kataoka, and Yutaka Satoh. "Can spatiotemporal 3d cnns retrace the history of 2d cnns and imagenet?." *Proceedings of the IEEE conference on Computer Vision and Pattern Recognition*. 2018.
- [46] Sun, Wei, et al. "A deep learning based no-reference quality assessment model for ugc videos." *Proceedings of the 30th ACM International Conference on Multimedia*. 2022.
- [47] Narwaria, Manish, Weisi Lin, and Anmin Liu. "Low-complexity video quality assessment using temporal quality variations." *IEEE Transactions on Multimedia* 14.3 (2012): 525-535.
- [48] Deng, Jia, et al. "Imagenet: A large-scale hierarchical image database." *2009 IEEE conference on computer vision and pattern recognition*. Ieee, 2009.
- [49] Kay, Will, et al. "The kinetics human action video dataset." *arXiv preprint arXiv:1705.06950* (2017).
- [50] Kingma, Diederik P., and Jimmy Ba. "Adam: A method for stochastic optimization." *arXiv preprint arXiv:1412.6980* (2014).
- [51] Paszke, Adam, et al. "Automatic differentiation in pytorch." (2017).
- [52] Ghadiyaram, Deepti, et al. "In-capture mobile video distortions: A study of subjective behavior and objective algorithms." *IEEE Transactions on Circuits and Systems for Video Technology* 28.9 (2017): 2061-2077.
- [53] Nuutinen, Mikko, et al. "CVD2014—A database for evaluating no-reference video quality assessment algorithms." *IEEE Transactions on Image Processing* 25.7 (2016): 3073-3086.
- [54] Hosu, Vlad, et al. "The Konstanz natural video database (KoNViD-1k)." *2017 Ninth international conference on quality of multimedia experience (QoMEX)*. IEEE, 2017.
- [55] Gao, Yixuan, et al. "VDPVE: VQA Dataset for Perceptual Video Enhancement." *Proceedings of the IEEE/CVF Conference on Computer Vision and Pattern Recognition*. 2023.
- [56] Antsiferova, Anastasia, et al. "Video compression dataset and benchmark of learning-based video-quality metrics." *Advances in Neural Information Processing Systems* 35 (2022): 13814-13825.
- [57] Sinno, Zeina, and Alan Conrad Bovik. "Large-scale study of perceptual video quality." *IEEE Transactions on Image Processing* 28.2 (2018): 612-627.
- [58] Wang, Yilin, Sasi Inguva, and Balu Adsumilli. "YouTube UGC dataset for video compression research." *2019 IEEE 21st International Workshop on Multimedia Signal Processing (MMSp)*. IEEE, 2019.
- [59] Yu, Xiangxu, et al. "Predicting the quality of compressed videos with pre-existing distortions." *IEEE Transactions on Image Processing* 30 (2021): 7511-7526.
- [60] Zhu, Wenhan, et al. "Multi-channel decomposition in tandem with free-energy principle for reduced-reference image quality assessment." *IEEE Transactions on Multimedia* 21.9 (2019): 2334-2346.
- [61] Min, Xionghuo, et al. "Objective quality evaluation of dehazed images." *IEEE Transactions on Intelligent Transportation Systems* 20.8 (2018): 2879-2892.
- [62] Min, Xionghuo, et al. "Quality evaluation of image dehazing methods using synthetic hazy images." *IEEE Transactions on Multimedia* 21.9 (2019): 2319-2333.
- [63] Krasula, Lukáš, et al. "On the accuracy of objective image and video quality models: New methodology for performance evaluation." *2016 Eighth International Conference on Quality of Multimedia Experience (QoMEX)*. IEEE, 2016.
- [64] Hanhart, Philippe, et al. "How to benchmark objective quality metrics from paired comparison data?." *2016 Eighth International Conference on Quality of Multimedia Experience (QoMEX)*. Ieee, 2016.
- [65] Krasula, Lukáš, et al. "Quality assessment of sharpened images: Challenges, methodology, and objective metrics." *IEEE Transactions on Image Processing* 26.3 (2017): 1496-1508.
- [66] Krasula, Lukáš, et al. "Preference of experience in image tone-mapping: Dataset and framework for objective measures comparison." *IEEE Journal of Selected Topics in Signal Processing* 11.1 (2016): 64-74.
- [67] Brill, Michael H., et al. "Accuracy and cross-calibration of video quality metrics: new methods from ATIS/T1A1." *Signal Processing: Image Communication* 19.2 (2004): 101-107.
- [68] Hanley, James A., and Barbara J. McNeil. "A method of comparing the areas under receiver operating characteristic curves derived from the same cases." *Radiology* 148.3 (1983): 839-843.
- [69] Korhonen, Jari. "Two-level approach for no-reference consumer video quality assessment." *IEEE Transactions on Image Processing* 28.12 (2019): 5923-5938.
- [70] Li, Dingquan, Tingting Jiang, and Ming Jiang. "Quality assessment of in-the-wild videos." *Proceedings of the 27th ACM International Conference on Multimedia*. 2019.
- [71] Sun, Wei, et al. "A deep learning based no-reference quality assessment model for ugc videos." *Proceedings of the 30th ACM International Conference on Multimedia*. 2022.
- [72] Wu, Haoning, et al. "Fast-vqa: Efficient end-to-end video quality assessment with fragment sampling." *European Conference on Computer Vision*. Cham: Springer Nature Switzerland, 2022.



**Zehao Zhu** received the B.E. degree in electronic information engineering from Jilin University in 2018 and the M.E. degree in information and communication engineering from Shanghai Jiao Tong University in 2021. He is currently pursuing the Ph.D. degree in electronic engineering with Shanghai Jiao Tong University, Shanghai, China. His research interests include streaming media quality of experience assessment and video quality assessment.



**Wei Sun** received the B.E. degree from the East China University of Science and Technology, Shanghai, China, in 2016, and the Ph.D. degree from Shanghai Jiao Tong University, Shanghai, China, in 2023. He is currently a Post-Doctoral Fellow with Shanghai Jiao Tong University. His research interests include image quality assessment, perceptual signal processing and mobile video processing.



**Jun Jia** received the B.S. degree in computer science and technology from Hunan University, Changsha, China, in 2018. He is currently pursuing the Ph.D. degree in electronic engineering with Shanghai Jiao Tong University, Shanghai, China. His current research interests include computer vision and image processing.



**Wei Wu** received his Ph.D. in computer application technology from Wuhan University, Wuhan, China, in 2021. He joined Donghai Laboratory in 2023. Before joining Donghai Laboratory, he was a Senior Engineer with Alibaba Group, Hangzhou, China, from 2021 to 2023. His research interests include image and video processing, computer vision, and multi-source heterogeneous data fusion.



**Jia Wang** received the B.Sc. degree in electronic engineering, the M.S. degree in pattern recognition and intelligence control, and the Ph.D. degree in electronic engineering from Shanghai Jiao Tong University, China, in 1997, 1999, and 2002, respectively. He is currently a Professor with the Department of Electronic Engineering, Shanghai Jiao Tong University, and also a member of the Shanghai Key Laboratory of Digital Media Processing and Transmission. His research interests include multiuser information theory and mathematics in artificial intelligence.



**Ying Chen** (IEEE M'05 - SM'11) received a B.S. in Applied Mathematics and an M.S. in Electrical Engineering & Computer Science, both from Peking University, in 2001 and 2004 respectively. He received his PhD in Computing and Electrical Engineering from Tampere University of Technology (TUT), Finland, in 2010. Dr. Chen joined Alibaba Group, in 2018 as a Senior Director. Before joining Alibaba. His earlier working experiences include Principal Engineer in Qualcomm Incorporated, San Diego, CA, USA from 2009 to 2018, Researcher in TUT and Nokia Research Center, Finland from 2006 to 2009 and Research Engineer in Thomson Corporate Research, Beijing, from 2004 to 2006. Dr. Chen is currently leading the Audiovisual Technology Group in Taobao, Alibaba, supporting end-to-end multimedia features and applications within Taobao. Dr. Chen has been focusing on algorithm development and commercialization of multimedia technologies. Dr. Chen contributed to three generations of video coding standards, H.264/AVC, H.265/HEVC, and H.266/VVC (earlier stage) and video file format and transport standards, with various technical contribution documents (500+). Dr. Chen has served as an editor and a software coordinator for H.264/AVC and H.265/HEVC (both for Multiview and 3D Video extensions). Dr. Chen's research areas include video coding, image/video restoration and enhancement, image/video quality assessment and video transmission. Dr. Chen has authored or co-authored 80+ academic papers and over 250 granted US patents in the fields of image/video processing and coding, multimedia transmission and computer vision. His publications have been cited for more than 20000 times. Dr. Chen has served as an associate editor for IEEE Transactions on CSVT.



**Guangtao Zhai** (Senior Member, IEEE) received the B.E. and M.E. degrees from Shandong University, Shandong, China, in 2001 and 2004, respectively, and the Ph.D. degree from Shanghai Jiao Tong University, Shanghai, China, in 2009. From 2008 to 2009, he was a Visiting Student with the Department of Electrical and Computer Engineering, McMaster University, Hamilton, ON, Canada, where he was a Post-Doctoral Fellow, from 2010 to 2012. From 2012 to 2013, he was a Humboldt Research Fellow with the Institute of Multimedia Communication and Signal Processing, Friedrich-Alexander-University of Erlangen-Nürnberg, Germany. He is currently a Research Professor with the Institute of Image Communication and Information Processing, Shanghai Jiao Tong University. His research interests include multimedia signal processing and perceptual signal processing. He received the Award of National Excellent Ph.D. Thesis from the Ministry of Education of China in 2012.